Applied Catalysis A: General 489 (2015) 255–261

Contents lists available at ScienceDirect

Applied Catalysis A: General

journal homepage: www.elsevier.com/locate/apcata

Photocatalytic inhibition of bacteria by TiO_2 nanotubes-doped polyethylene composites

Daniela Yañez[a,b], Sichem Guerrero[c], Ingo Lieberwirth[d], María Teresa Ulloa[e], Tatiana Gomez[f], Franco M. Rabagliati[a], Paula A. Zapata[a,*]

[a] Grupo Polímeros, Facultad de Química y Biología, Universidad de Santiago de Chile, USACH, Casilla 40, Correo 33, Santiago, Chile
[b] Departamento de Ciencias Químicas, Facultad de Ciencias Exactas, Universidad Andrés Bello, Republica 275, Santiago, Chile
[c] Facultad de Ingeniería y Ciencias Aplicadas, Universidad de los Andes, Monseñor Álvaro del Portillo 12455, Las Condes, Santiago, Chile
[d] Max Planck Institute Polymer Research, 55128 Mainz, Germany
[e] Programa de Microbiología y Micología, ICBM-Facultad de Medicina Universidad de Chile, Independencia, Chile
[f] Dirección de Postgrado e Investigación, Universidad Autonoma de Chile, Carlos Antúnez 1920, Santiago, Chile

ARTICLE INFO

Article history:
Received 12 August 2014
Received in revised form 22 October 2014
Accepted 26 October 2014
Available online 3 November 2014

Keywords:
Nanocomposites
Polyethylene
TiO_2 nanotubes
Photocatalytic inhibition

ABSTRACT

Polyethylene (PE) and polyethylene-octadecene (LLDPE) composites containing titanium dioxide nanotubes were synthesized and applied to the inhibition of selected bacteria. It was found that polymerization rate of the polymerizations increased with the incorporation of the octadecene compared with bare ethylene, while with modified nanotubes (O–TiO_2–Ntbs) the catalytic activity showed a slight decrease compared with the pure polymer. Regarding physical properties, the melting temperature and cristallinity of PE was higher than LLDPE. LLDPE presented lower rigidity than PE and thus lower Young's modulus. On the other hand, with the incorporation of nanotubes, Young's modulus did not change significantly with respect to PE. After 2 h of contact, the PE/O–TiO_2–Ntbs composite showed a reduction of *Escherichia coli* of 36.7% under no UVA irradiations. In contrast, LLDPE/O–TiO_2–Ntbs showed 63.5%. The photocatalytic reduction (under UVA light) was much higher and after 60 min the LLDPE/*O*-TiO_2-Ntbs composites showed a bacterial reduction of 99.9%, whereas the PE/*O*-TiO_2-Ntbs showed 42.6% of catalytic reduction.

1. Introduction

Nanocomposites have gained attention due to their interesting properties and because the incorporation of low amounts of nanoparticles can enhance the mechanical, optical, catalytic, and thermal properties, among others. The catalytic biocidal properties of nanocomposite materials constitute an attractive alternative to be used in the medical and food packaging fields. In order to obtain catalytic biocidal properties, different nanoparticles such as silver [1], copper [2], and recently TiO_2 nanoparticles [3] have been incorporated into polyolefins. TiO_2 nanoparticles possess odor inhibition and self-cleaning mechanisms. Furthermore, they are inert, nontoxic and inexpensive materials, with a high refractive index and a high ability to absorb UV light. TiO_2 excited by light with a radiation input greater than the particular band gap energy of the TiO_2 crystal (3.2 eV for anatase; 3.03 eV for rutile) generate pairs of holes (h^+) and electrons (e^-) by molecular excitation, which can migrate to the surface of the catalyst to react with water and oxygen generating hydroxyl radicals (OH•) and reactive oxygen species able to degrade cell components of microorganism and act as anti-bacterial agents.

Due to their better physical properties as barriers and their good mechanical properties, high density and low density polyethylene and polypropylene are the most commonly used polymeric materials for packaging applications. It is known that the direct application of antibacterials on the surface of foods is limited because the active agent may diffuse into the food itself [4]. The advantage of a polymer matrix is that the nanoparticles that give the catalytic biocidal properties are always retained by the polymer, which protects the food at all times. Usually, TiO_2 nanoparticles with spherical morphology had been used as fillers on polypropylene and polyethylene by the casting and melting processes in order to confer biocidal properties.

In other studies [5,6], TiO_2 nanoparticles ca. 7 nm in diameter were embedded into a polypropylene (PP) matrix using a casting method, leading to the formation of an oriented polypropylene

* Corresponding author. Tel.: +56 2 27181149.
E-mail address: paula.zapata@usach.cl (P.A. Zapata).

http://dx.doi.org/10.1016/j.apcata.2014.10.051
0926-860X/

plastic (OPP). This OPP showed catalytic biocidal effects against *Escherichia coli* and fungicidal properties against *Penicillium expansum* in lettuce packaging under UV illumination. The extent of inactivation of bacteria and fungi in a TiO_2 film presented high efficacy when the films were irradiated with UVA light with an intensity of 1 mW/cm^2. Below this intensity the efficacy decreased noticeably and it was correlated with higher OH• radical formation on the TiO_2 surface. However, the amount of TiO_2 incorporated into the oriented OPP was not reported. In another study [7], PP/TiO_2 nanocomposites were obtained using the hydrolysis-condensation reaction (sol–gel method) of titanium alkoxide premixed with PP using the melting process. The sol–gel method caused good TiO_2 dispersion (9.6 wt%) throughout the polymer matrix. These samples exhibited higher biocidal activity against *Staphylococcus aureus* and *E. coli* in the absence of light after 24 h than those obtained through the dispersion of the anatase phase in the molten PP. The authors attributed the results to the smaller particle size obtained by sol–gel method (ca. 10 nm diameter) and to the improved dispersion of the nanoparticles compared with traditional molten PP with TiO_2.

Kubacka et al. [8] reported the incorporation of TiO_2 nanoparticles (ca. 10 nm in size) into isotactic polypropylene (i-PP/TiO_2) by the melting process. Biocidal catalytic properties of the i-PP/TiO_2 nanocomposite films were obtained against Gram-negative and Gram-positive bacteria. TiO_2 showed maximum activity against bacteria with a load of 2 wt% of anatase-TiO_2. On the other hand, the i-PP/TiO_2 nanocomposites were completely inactive against bacteria under dark conditions. The authors explained this behavior by the absence of the oxide on the surface of the material.

Altan et al. [9] prepared PP/TiO_2 nanocomposites by melt compounding. In order to avoid the agglomeration of particles, the authors used two methods to modify the nanoparticles: one was by coating the TiO_2 with an elastomeric phase based on maleic anhydride grafted to styrene-ethylene-butylene-styrene (SEBS-*g*-MA) and silane compounds, and the other method was by coating the nanoparticles only with silane groups. The SEBS-*g*-MA and silane-coated TiO_2 nanoparticles provided higher mechanical and biocidal properties than TiO_2 nanoparticles modified with silane. The catalytic biocidal efficiency was related to the particles' dispersion. They found that the composites with low TiO_2 content showed higher antibacterial properties based on the better photocatalytic activity of the particles during UV irradiation.

Xing et al. [4] prepared polyethylene nanocomposites with 2 wt% TiO_2 nanoparticle content (ca. 10–20 nm particle size) using a blender mixer. The PE/TiO_2 nanocomposite films presented biocidal properties with an inhibition ratio of 50.4% for *E. coli* and 58.0% for *S. aureus* without UV. The inhibition ratio improved significantly with UV irradiation of PE/TiO_2 films, reaching 89.3% for *E. coli* and 95.2% for *S. aureus*. The mechanical properties improved with the incorporation of the TiO_2 nanoparticles. In a similar approach, Li et al. [10] obtained a novel nano-packaging for Chinese jujube by blending polyethylene (56%) with a nano-powder mix (30%) (silver, clay and anatase TiO_2, rutile TiO_2), and crosslinking reagents (14%). The results showed that the film with nanoparticles had a quite beneficial effect on the physicochemical and sensory quality compared with normal packing materials. After 12 days of storage, fruit softening, weight loss, browing and climatic evolution of nano-packaging were significantly inhibited. However, biocidal properties were not studied in that work.

The catalytic biocidal properties are related with the dispersion of nanoparticles into the polymer matrix. Therefore, our group proposed a procedure in order to improve the dispersion of the nanoparticles by an in situ polymerization in which the ethylene polymerization was carried out in the presence of the TiO_2 nanospheres (PE/TiO_2) and this organic modified with silane compound (PE/Mod-TiO_2) PE/TiO_2 nanocomposites containing 8 wt% TiO_2 nanospheres exposed to UVA irradiations presented a high antimicrobial activity against *E. coli*. In fact, the PE/Mod-TiO_2 nanocomposite with 8 wt% filler eliminated 99.99% of *E. coli* regardless of light and time of irradiation [3].

No reports using TiO_2 nanotubes for obtaining PE nanocomposites having catalytic biocidal character have been reported so far in the literature. Therefore, in this paper we propose studying the catalytic biocidal properties against *E. coli* when 5 wt% of TiO_2 nanotubes are incorporated in polymer matrices with different crystallinity (polyethylene: PE and polyethylene-octadecene: LLDPE). In order to improve the interaction with the non-polar matrix, the TiO_2 nanotubes were organically-modified with oleic acid and the nanocomposites were obtained by in situ polymerization. The catalytic activity of the system and the thermal, mechanical, and antimicrobial properties against *E. coli* of the PE/*O*-TiO_2-Ntbs and LLDPE/*O*-TiO_2-Ntbs nanocomposites are presented.

2. Experimental

2.1. Materials

TiO_2 nanotubes were synthesized by a hydrothermal method previously reported [3]. Briefly, the reagents used were nitric acid (HNO_3), sodium hydroxide (NaOH) pellets (Mallinckrodt, Chemicals), and distilled water. Oleic acid (Aldrich, reagent grade, 98%) was used for the modification of the TiO_2 nanotubes.

The polymerization reactions, described in detail in a previous work, used ethenyl(bisindenyl)zirconium dichloride (rac-$EtInd_2ZrCl_2$) as catalyst and methylaluminoxane (MAO) (Chemtura Europe GmbH, 10% solution in toluene) as cocatalyst [1]. 1-Octadecene (Aldrich, reagent grade, 90%) was used for the ethylene-*co*-1-octadecene copolymerizations.

2.2. Preparation of titanium oxide nanotubes (TiO_2Ntbs)

The precursor from nanotubes were TiO_2 nanospheres synthesized by a sol–gel method [3]. The nanotubes were obtained by the hydrothermal method reported in a previous paper [11,12]. TiO_2 nanospheres (2.5 g) were mixed with 125 mL NaOH (10 M), and the mixture was then placed in a Teflon closed-vessel at 110 °C for 24 h, stirring every hour. Afterwards, the obtained slurry was washed several times with distilled water (4 L) and then filtered to separate the powder. Next, 150 mL of 0.1 M HNO_3 were added to the powder and mixed for 24 h. The slurry was washed with 1 L of distillated water. Finally, the filtered nanoparticles were calcined at ca. 200 °C for 4 h.

2.3. Organic modification of titanium oxide nanotubes (*O*-TiO_2Ntbs)

The nanoparticles were modified with oleic acid using the method reported by Li and Zhu [13]. 1-Hexane (100 mL) and oleic acid (200 μL) were mixed with stirring. Then 1 g of TiO_2-Ntbs was added to the solution under at 60 °C with vigorous stirring during 5 h. The nanoparticles were filtered, washed with ethanol, and vacuum-dried at 100 °C during 24 h. Before being used in the polymerization reactions, the obtained *O*-TiO_2-Ntbs particles were sonicated in toluene under an inert atmosphere during 10 min in a 130 Watt Ultrasonic Processor with a Thumb Actuated pulser equipped with a 6 mm diameter tip.

2.4. Polymerization of ethylene, ethylene-1-octadecene, and nanocomposites

Ethylene homopolymer and LLDPE (0.16 mol/L octadecene) copolymers were synthesized using the metallocene catalyst rac-ethenyl(bisindenyl) zirconium dichloride (rac-$EtInd_2ZrCl_2$). The

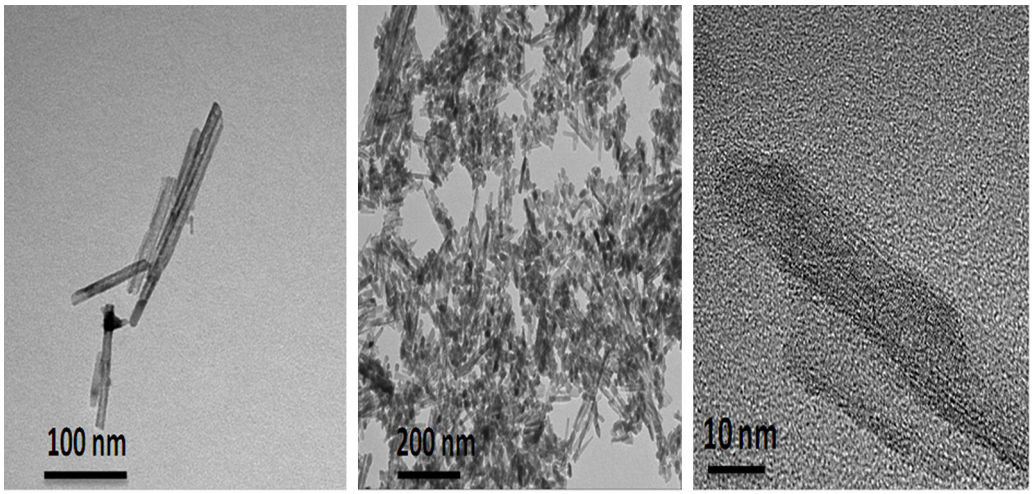

Fig. 1. TEM images of TiO_2 nanotubes.

polymerization reactions were carried out in a Parr glass reactor (400 mL) with temperature control (60 °C) and mechanical stirring (500 rpm). Toluene (90 mL) and MAO (4.32×10^{-3} mol) were used, and in the case of the copolymerizations 5 mL of 1-octadecene (0.16 mol/L) were added to the reactor. Then, the metallocene catalyst solution in toluene (3×10^{-6} mol) was also added. Finally the system was saturated with ethylene at 1 bar of pressure during 30 min. For the nanocomposite preparations, the preparation was performed under the same reaction conditions used for ethylene. In that case, 5 wt% of modified nanotubes were added to the reactor and mixed with MAO for 2 min. Then 1-octadecene (in the case of copolymerizations) and the catalyst were added, and finally the mixture was saturated with ethylene. Acidified methanol (10% HCl, 10 mL) was added to stop the reaction. The solid polymer product was recovered by filtration, washed with methanol, and then dried overnight at room temperature. The rate of polymerization is expressed as the mass of PE (kg) produced per unit time (h) per mol of Zr and per unit pressure (kg/mol/bar/h). All the polymerization reactions were repeated to verify reproducibility. The nanocomposites are designated as PE/*O*-TiO_2-Ntbs, while those obtained by copolymerization are identified as LLDPE/*O*-TiO_2-Ntbs.

2.5. Composite characterization

The XRD patterns of the TiO_2 nanotubes were obtained on a Siemens D5000 diffractometer, using Ni-filtered Cu $K\alpha$ radiation ($\lambda = 0.154$ nm).

UV absorption spectra of the *O*-TiO_2-NTbs nanotube powders were measured on a Perkim Elmer Lambda 650 UV/Vis spectrometer. The UV spectra measurements were conducted within the 200–700 nm range. The band gap (E_g) energies were calculated according to the equation $E_g = 1239.6/\lambda_g$ [14].

Diffuse reflectance infrared Fourier-transform (DRIFT) analysis of the titanium oxide and modified titanium nanoparticles was performed on a Bruker Vector 22 FTIR spectrometer with Harrick diffuse reflectance. The DRIFT spectra were collected in the 4000 to 500 cm^{-1} range, with a resolution of 4 cm^{-1} at room temperature.

The melting temperature and enthalpy of fusion of the neat polymer and nanocomposites samples were measured by differential scanning calorimetry (DSC) (TA Instruments DSC 2920). The samples were heated from 25 °C to 180 °C at a rate of 10 °C/min and then cooled to 25 °C at the same rate; the values were taken from the first heating curve [15]. Percent crystallinity was calculated using the enthalpy of fusion of an ideal polyethylene with 100% crystallinity (289 J/g) accordingly to Wei et al. [16].

Polymer viscosity was measured in *o*-dichlorobenzene at 135 °C in a Viscosimatic-Sofica viscometer.

The polymer's thermal stability was evaluated by thermogravimetric analysis (TGA) using a Netzsch TG Libra 209 instrument in an inert atmosphere (nitrogen). The samples were heated from 25 °C to 600 °C at a rate of 20 °C/min.

The morphology of the TiO_2-Ntbs and their dispersion in the composites were analyzed by TEM (JEOL ARM 200 F) operating at 20 kV. Samples for TEM measurements were prepared by placing a drop of TiO_2-NTbs on a carbon-coated standard copper grid (400 mesh) and evaporating the solvent. Ultra-thin polyethylene nanocomposite specimens with a thickness of ca. 100 nm were cut with glass blades in an ultra-microtome at −40 °C.

The tensile properties of the polymer and composites were determined on an HP model D-500 dynamometer. The materials were molded for 3 min in a hydraulic press, HP Industrial Instruments, at a pressure of 50 bar and 170 °C, and further cooled under pressure with water circulation. Films around 0.05 mm thickness were obtained. Dumbbell-shaped samples with an effective length of 30 mm and a width of 5 mm were cut from the compression-molded sheets. The samples were tested at a rate of 50 mm/min at 20 °C. Each set of measurements was repeated at least four times.

2.6. Biocidal properties

The catalytic antimicrobial effect of the different samples was determined using a plate count method described by the ISO 20143. *E. coli* ATCC 25922 was used for analysis. In brief, the initial number of bacteria present after incubation was calculated by counting the number of colonies in a ten-fold dilution. From a fresh culture, a microbial suspension of 1×10^7 CFU/mL by densimat BioMérieux® was prepared in a BHI broth plus Triton 100× in a humid chamber. The suspension, 0.5 mL, was placed in contact with every 2.5 cm^2 sample (pure PE and LLPDE as control, and PE/TiO_2-NTbs and LLPDE/TiO_2-NTbs) for 60, 120, and 240 min. Then, each sample was exposed to white light and UVA light using two 8 W black light bulbs, Hitachi (FL-8BL-B). The UVA (315–400 nm) light intensity was 0.2 mW/cm^2 as measured by a digital light meter (SLM-110, A.W. Sperry). Each sample (control and antibacterial-treated) was recovered by suspending in 10 mL of sterile saline solution and then diluted serially down to 1/10, 1/100, and 1/1000. Then, 0.2 mL of each dilution was plated in duplicate on trypticase soy agar plates and incubated at 37 °C for 24 h. After incubation, the number of colonies in the Petri dishes was counted and in this way the percentage of inhibition of microorganism in each sample was determined

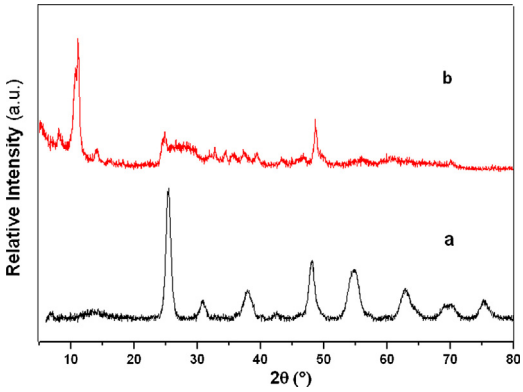

Fig. 2. XRD diffraction spectra of (a) TiO_2 nanospheres and (b) *O*-TiO_2-Ntbs.

compared to its corresponding control. The percent reduction of the colonies was calculated using the following equations, which relate the number of colonies from the neat polymer with the number of colonies from the nanocomposites.

$$\%R = \frac{\text{CFU neat polymer} - \text{CFU nanocomposite}}{\text{CFU neat polymer}} \times 100$$

3. Results and discussions

3.1. Characterization of titanium oxide nanotubes (TiO_2-NTbs and O-TiO_2-NTbs)

The nanoparticle morphology was studied by transmission electron microscopy (TEM) and it is shown in Fig. 1. The nanoparticles have nanotube morphology with average diameters of ca. 20 nm and a length of ca. 500 nm. The images showed a few nanospheres around the nanotubes. The crystalline phase of the raw materials and nanotubes were studied by XRD (Fig. 2). Nanospheres and nanotubes presented two characteristic Bragg reflections from the anatase phase corresponding to tetragonal crystal planes (1 0 1) and (2 0 0), located at 25° and 48°, respectively [17,18]. In the case of nanotubes a new peak appears at 11° corresponding to phases of titanate nanotubes [19,20].

The method used for the organic modification of nanoparticles reported by Li and Zhu [13] was verified by the DRIFT spectra, where the peaks corresponding to the alkyl chain of oleic acid appeared at 2920 cm^{-1} and 2855 cm^{-1} (Fig. 3). The disappearance of the peak at 1710 cm^{-1} indicates that the oleic acid group,–COOH, has reacted with surface hydroxyl groups from TiO_2. The peaks at 1590 cm^{-1} correspond to carboxylate groups, and the peaks at 1550 cm^{-1} and 1430 cm^{-1} indicate the presence of —COO^- [21].

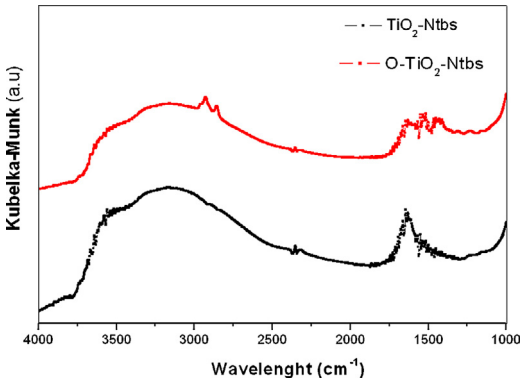

Fig. 3. DRIFT spectra of (a) nanotubes and (b) modified nanotubes with oleic acid (*O*-TiO_2-Ntbs).

Table 1
Wavelength and energy "Band gap" (eV) of nanospheres (raw materials) and nanotubes.

Sample	Wavelength (nm)	Energy* (eV)
TiO_2-nanosphere	402	3.08
TiO_2-Ntbs	387	3.20
O-TiO_2-Ntbs	392	3.16

* Values of energy obtained by $E_g = 1239.6/\lambda_g$ [22].

Table 1 shows the wavelength values and energy band gap obtained by UV absorption on TiO_2 nanospheres (raw materials) and nanotubes before and after modification with oleic acid. These values are related to the band transition of valence electrons characteristic of TiO_2 [22,23]. The nanospheres presented an energy band gap (E_g) of 3.08 eV characteristic of the anatase phase. On the other hand and as expected, the change of the morphology into TiO_2 nanotubes led to an increased of the energy band gap up to 3.20 eV. In the case of *O*-TiO_2-Ntbs, the organic modification with oleic acid gave place to an energy band gap of 3.16 eV.

3.2. Rate of homopolymerization and copolymerization in the presence of titanium nanotubes

The influence of the incorporation of *O*-TiO_2-Ntbs on the rate of homopolymerization and copolymerization is shown in Table 2. The first effect observed is already known and it is related to the increased rate with larger amounts of octadecene in the feed. The incorporation of the comonomer increases the solubility of the monomer in the liquid phase, and consequently increases the insertion rate. Moreover, the higher solubility of the copolymer reduces the monomer's diffusion limitations toward active centers [24]. On the other hand, when 5 wt% of oleic-acid-modified nanotubes were incorporated, the rate decreased slightly with this effect being more pronounced for copolymerization. Although it is not clear at the moment, we speculate that this decrease in the rates of polymerization may be due to the possible deactivation of the metallocene by oleic acid, or to the fact that the nanotubes prevent the insertion of the comonomer on the active sites due to steric hindrance by the nanotube morphology. We have previously studied the incorporations of TiO_2 nanospheres modified with silane (Mod-TiO_2) in ethylene polymerization, where an increase in the rates was found in the presence of Mod-TiO_2. This behavior was explained by the role of silane acting as a spacer, thus hindering the bimolecular deactivation between neighboring zirconocenes in the solution, and thereby having a positive effect on the rates of polymerization. In the same work, the results for the copolymerization of LLDPE indicated that the presence of mod-TiO_2 did not affect the polymerization rate [3,17].

3.3. Polymer characterization

Viscosity is related to the molecular weight of the polymer, and it decreased with the incorporation of comonomer and nanoparticles. This effect can be due to the increase of transfer reactions with comonomer incorporation or nanotube addition to the reactor [25]. As expected with the comonomer incorporation, both the melting temperature and cristallinity of polyethylene decreased (see Table 3). These changes could be explained by the role of octadecene branches, which hinder crystallization because octadecene is excluded from the crystal lattice of polyethylene [24,26]. The melting temperature and crystallinity of the nanocomposites did not change compared with the pure polymers.

Table 2
Catalytic activity of the ethylene and *co*-(ethylene-1octadecene) polymerizations in the presence of the *O*-TiO_2-Ntbs.

Samples	TiO_2-Ntbs content (wt.%)	Octadecene feed (mol/L)	Catalytic activity (kg/mol/Zr/h/bar)	[η] (dL/g)
PE	0	0.00	2170	2.16
PE/*O*-TiO_2-Ntbs	5	0.00	1933	2.02
LLDPE	0	0.16	5040	1.07
LLDPE/*O*-TiO_2-Ntbs	5	0.16	4267	0.66

T_p: polymerization temperature. η: viscosity. Polymerization conditions: mol Zr: 3×10^{-6}; Al/Zr: 1400: 60 °C. Pressure: 1 bar; reaction time: 30 min.

Table 3
Thermal properties and Young's modulus (E) of PE/TiO_2-Ntbs and LLDPE/TiO_2-Ntbs nanocomposites.

Samples	TiO_2-Ntbs (wt.%)	Tm_1	X_c (%)	T_{10} (°C)	T_{max} (°C)	E (Mpa)
PE	0	138	53	451	488	608 ± 45
PE/*O*-TiO_2-Ntbs	5	136	52	449	478	529 ± 77
LLDPE	0	115	3	432	469	11 ± 3
LLDPE-1/*O*-TiO_2-Ntbs	5	105	2	417	464	9 ± 0.8

T_{m1}: melting temperature, first heating; X_c: percent crystallinity. T_{10}: decomposition temperature at 10% weight loss, T_{max}: temperature for the maximum rate of weight loss (T_{peak}). E = Young's modulus.

The thermal stability of the polymers was studied by TGA under a nitrogen atmosphere, as shown in Table 3. T_{10} and T_{max} decreased with the incorporation of nanotubes. According to the literature, the incorporation of titanium nanoparticles leads to an enhancement of the thermal stability and maximum decomposition temperature of the nanocomposites compared with virgin polymers [17]. But in our case the decrease in the thermal stability (ca. 10 °C) is due to the use of oleic acid as modifier. In fact, oleic acid starts degrading at around 150 °C, and this can contribute to destabilizing the polymer matrix [27]. The elastic modulus for neat polymer and the nanocomposites is also reported in Table 3. The crystallinity and crystal structure affect the mechanical properties, and as the polymer's crystallinity decreases its flexibility increases. With the incorporation of comonomer to promote branching, the polymer's ability to absorb and dissipate energy also increases. Cristillanity decreases with the addition of comonomer, which is related with the elastic modulus that also decreases, and therefore the rigidity of the polymer also decreases [28]. On the other hand, the elastic modulus of the polymers did not undergo any change with the incorporation of nanoparticles.

TEM images of the PE/*O*-TiO_2-Ntbs containing 5 wt% of filler are shown in Fig. 4. In general, TiO_2 nanoparticles in the PE matrix were well distributed, which is due to the organic modifications of the surface of nanoparticles. This modification improved the adhesion between the nanoparticles and the polymer matrix. Nevertheless, TEM images also showed some minor zones with particle agglomeration.

Table 4
Reduction percentage of the *E. coli* of PE/*O*-TiO_2 and LLDPE/*O*-TiO_2 nanocomposites.

Samples	Irradiation time (min)	% Bacteria reduction	
		White light	UV light
PE/*O*-TiO_2-Ntbs	60	28.2	42.6
	120	36.7	43.1
LLDPE/*O*-TiO_2-Ntbs	60	43.1	99.7
	120	63.5	99.9
	240	98.2	99.9

3.4. Catalytic biocidal properties and discussion

The catalytic biocidal properties of the polymers against *E. coli* are shown in Table 4 and Fig. 5. The polymers were irradiated with UV light and compared with white light irradiation over different times. The catalytic activity expressed as reduction percentages were calculated based on the polymer without nanoparticles as reference. Two different factors determined the biocidal properties of the materials: the irradiation source and the type of polymer matrix

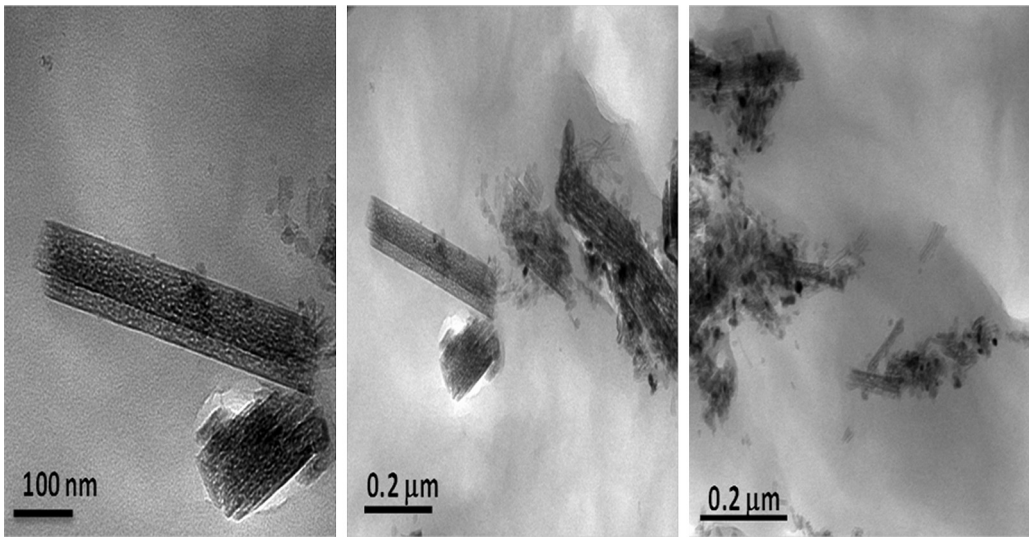

Fig. 4. TEM images of the PE/*O*-TiO_2-Ntbs nanocomposites.

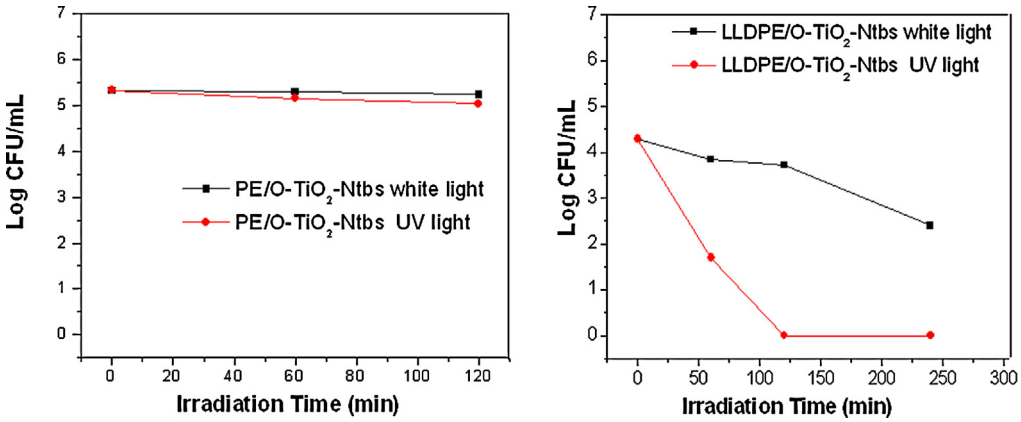

Fig. 5. Biocide properties of the PE/*O*-TiO_2-Ntbs and LLDPE/*O*-TiO_2-Ntbs.

used. As expected, the catalytic biocidal properties depended on the irradiation source. When using UV irradiation, the nanocomposites had a greater reduction of *E. coli* than when a white light source was used. This biocidal effect was more pronounced for the LLDPE/TiO_2 nanocomposite, achieving a reduction of ca. 99.99%. The mechanism of photoreduction of *E. coli* on TiO_2 is ascribed to the irradiation with UV light ($\lambda < 387$ nm), which generates electron and hole pairs. The created electrons and reactive oxygen will combine into O_2^-, and the positive electric holes and water generate hydroxyl radicals (OH•) and hydroperoxy radicals (HOO•) [29]. During the initial reactions the reactive species cause a partial decomposition of the outer cell membrane, changing its permeability. After that, the reactive species can easily reach the cytoplasmic membrane, leading to its peroxidation followed by the death of the cells [30]. Sunada et al. [31], studied the decomposition of the wall of bacteria by measuring the concentration of lipopolysaccharides (LPS) with irradiation time. They found a slight increase of LPS concentration during the initial slow step of intact cell death. This increase suggests that the outer membrane is decomposed by photocatalysis. By subsequent irradiation, LPS concentration decreased, indicating that free and fixed LPS were decomposed by a photocatalytic reaction. Another relevant aspect is the intensity of UVA light. Chawengkijwanich et al. [5] reported that when light intensity decreased from 1 to <0.05 mW/cm^2, the antimicrobial efficacy decreased. Such effect can be related to OH• radical concentration. In our case, the UVA light intensity was 0.2 mW/cm^2. The catalytic reduction of *E. coli* on PE/*O*-TiO_2-Ntbs under this UVA radiation was 43.2%. This low activity compared to other reports may be due to the low light intensity used here. On the other hand, a certain degree of biocidal character was still found in our nanocomposites when UV irradiation was not used. In fact, the LLDPE/*O*-TiO_2-Ntbs samples reach a reduction against *E. coli* of ca. 63.5% after 120 min, which increased to 98.2% after 240 min of contact time without UV irradiations. Li et al. [4] postulated that microorganisms carry a negative charge, while metal oxides carry a positive charge. This difference in charge creates "electromagnetic" attractions between the microbe and the surface. When contacting the surface the microbes release ions, which react with the thiol groups of the proteins present on the surface of the bacteria. On the other hand, different authors have reported the inhibition of *E. coli* on TiO_2 in the absence of light. In the absence of photoactivation, TiO_2 may induce an increase in oxidative stress correlated with the hydrogen peroxide concentration and with small particles of the TiO_2 [32,33].

The second effect is related to the crystallinity of the matrix used. For PE/*O*-TiO_2-Ntbs nanocomposites, the reduction percentage increased slightly with white light irradiations up to ca. 36.7% after 120 min. On the other hand, the LLDPE/*O*-TiO_2-Ntbs nanocomposites showed increased biocidal properties, which in turn were dependent on exposure time. After 240 min of irradiation the LLDPE/*O*-TiO_2-Ntb nanocomposites showed an increase of their biocidal properties up to a reduction of 98.2%. The latter is an important result that shows that these type of composites has the potential to be used in practical applications no requiring UV irradiation such as for example food packaging.

When nanocomposites were irradiated with UV, the reduction was independent of time. For PE/*O*-TiO_2-Ntb and LLDPE/*O*-TiO_2-Ntb nanocomposites, the reduction against *E. coli* after 2 h of exposure was 43.1% and 99.9%, respectively. This behavior can be ascribed to the higher crystallinity of PE when compared with LLDPE. In fact, the irradiated light can penetrate more easily in the amorphous zones of LLDPE. On the other hand, the nanoparticles can also travel more easily in the amorphous part of LLDPE than PE, which favors the nanoparticle diffusion to the surface of the film. Afterwards, in contact with oxygen and humidity, the active species are generated and therefore high biocidal properties against *E. coli* are observed.

In summary, there is an influence of the matrix used on the final biocidal properties. In our case, the catalytic biocidal activity was related to the crystallinity or morphology of the polymer used. Another important point is the morphology of the nanoparticles. In our study, nanotubes were used because their nanoparticles have a higher aspect ratio (length:diameter) than nanospheres, and therefore a higher biocidal efficiency was expected. This is because the morphology of the nanotubes delayed the recombination of electrons with the valence band compared to nanospheres. When unmodified nanospheres were incorporated in the polyethylene matrix by in situ polymerization with and without UV irradiation, the biocidal properties had a similar behavior as that of nanotubes [3]. The advantage of nanotubes is due to the high aspect ratio and to the possible decrease in the permeability to oxygen and water vapor. The latter is caused by the fact that nanotubes contribute to a more tortuous path for gases diffusing through the polymer matrix. It is also known that ethylene generated by some fruits is decomposed by TiO_2 nanoparticles [5,6]. These properties and all the results presented in this work suggest that these types of materials have a tremendous potential in food packaging applications.

4. Conclusions

Nanotubes were synthesized by a hydrothermal method from TiO_2 with spherical morphology, which in turn was used to obtain TiO_2 nanotubes modified organically with oleic acid (*O*-TiO_2-Ntbs).

PE/*O*-TiO_2-Ntbs and LLDPE/*O*-TiO_2-Ntbs nanocomposites were prepared by in situ polymerization. It was found that the type of matrix has an important influence on the biocidal properties

against *E. coli*. The LLDPE/*O*-Ntbs-TiO_2 nanocomposites had better biocidal activity compared to PE/*O*-Ntbs-TiO_2 nanocomposites. This behavior might be related to the degree of crystallinity of the polymer matrix. The increase in the amorphous character permits the migration of the nanoparticles to the surface and the generation of active OH• species causing the decomposition of the bacteria.

LLDPE/*O*-Ntbs-TiO_2 nanocomposites were highly effective against *E. coli* under UVA irradiation, and this effect was independent of time of exposure. The antimicrobial activity against *E. coli* reached 99.99%. On the other hand, for the same system without UV irradiation, the nanocomposites still showed a high efficacy against *E. coli*, with a reduction of ca. 98.2% after 240 min. Therefore, these systems are attractive when used as effective food packaging.

Acknowledgements

P.A. Zapata acknowledges the financial support under CONICYT insertion project 79100010, FONDECYT Project "Iniciación en Investigación 11110237" to P.A. Zapata, and DICYT-USACH Project 021341 RC. T.G. acknowledges financial support provided by project FONDECYT no. 3130530.

References

[1] P.A. Zapata, L. Tamayo, M. Páez, E. Cerda, I. Azocar, F.M. Rabagliati, Eur. Polym. J. 47 (2011) 1541–1549.
[2] H. Palza, S. Gutierrez, O. Salazar, V. Fuenzalida, J. Avila, G. Figueroa, R. Quijada, Macromol. Rapid Commun. 31 (2010) 563–567.
[3] P.A. Zapata, H. Palza, F.M. Rabagliati, J. Polym. Sci., A: Polym. Chem. 50 (2012) 4055–4062.
[4] Y. Xing, X. Li, L. Zhang, Q. Xu, Z. Che, W. Li, Y. Bai, K. Li, Composites, B: Eng. 45 (2013) 1192–1198.
[5] Ch. Chawengkijwanich, Y. Hayata, Int. J. Food Microbiol. 123 (2008) 288–292.
[6] Ch. Maneerat, Y. Hayata, Int. J. Food Microbiol. 107 (2006) 99–103.
[7] W. Bahloul, F. Mélis, V. Bounor-Legaré, P. Cassagnau, Mater. Chem. Phys. 134 (2012) 399–406.
[8] A. Kubacka, M. Ferrer, M.L. Cerrada, C. Serrano, M. Sánchez-Chaves, M. Fernández-García, A. de Andrés, R. Jiménez, F. Fernández-Martín, Appl. Catal., B: Environ. 89 (2009) 441–447.
[9] M. Altan, H. Yildirim, J. Mater. Sci. Technol. 28 (2012) 686–692.
[10] H. Li, F. Li, L. Wang, J. Sheng, Z. Xin, L. Zhao, H. Xiao, Y. Zheng, Q. Hu, Food Chem. 114 (2009) 547–552.
[11] T. Kasuga, M. Hiratmasu, A. Hoson, T. Sekino, K. Niihara, Adv. Mater. 11 (1999) 1307–1311.
[12] D. Salinas, P. Araya, S. Guerrero, Appl. Catal., B: Environ. 117-118 (2012) 260–267.
[13] Z. Li, Y. Zhu, Appl. Surf. Sci. 211 (2003) 315–320.
[14] M.I. Mejia, J.M. Marín, G. Restrepo, L.A. Rios, C.J. Pulgarín, Appl. Catal., B: Environ. 94 (2010) 166–172.
[15] C.L. Shan, J.B.P. Soares, A. Penlidis, Polymer 43 (2002) 767–773.
[16] L. Wei, T. Tang, B. Huang, J. Polym. Sci. A: Polym. Chem. 42 (2004) 941–949.
[17] P.A. Zapata, H. Palza, L.S. Cruz, I. Lieberwirth, F. Catalina, T. Corrales, F.M. Rabagliati, Polymer 54 (2013) 2690–2698.
[18] Sg. Ansari, M. Pazouki, A. Hosseinnia, Powder Technol. 196 (2009) 241–245.
[19] P.K. Khanna, N. Singh, S. Charan, Mater. Lett. 61 (2007) 4725–4730.
[20] J.-N. Nian, S.-A. Chen, C.-C. Tsai, H. Teng, J. Phys. Chem. B 110 (2006) 25817–25824.
[21] Y. Gao, G. Chen, Y. Oli, Z. Zhang, Q. Xue, Wear 252 (2002) 454–458.
[22] K. László, D. Imre, Colloids Surf., A: Physicochem. Eng. Aspects 280 (2006) 146–154.
[23] M.I. Mejia, J.M. Marín, G. Restrepo, L.A. Rios, C. Pulgarín, Appl. Catal., B: Environ. 94 (2010) 166–172.
[24] R. Quijada, A. Narváez, R. Rojas, F.M. Rabagliati, Barrera, G. Galland, R. Santos Mauler, R. Benavente, E. Pérez, J.M. Pereña, A. Bello, Macromol. Chem. Phys. 200 (1999) 1306–1310.
[25] R. Quijada, G. Barrera Galland, R.S. Mauler, Macromol. Chem. Phys. 197 (1996) 3091–3098.
[26] E. Kontuo, M. Niaounakos, G. Spathis, Eur. Polym. J. 38 (2002) 2477–2487.
[27] T. Sago, H. Ishii, H. Hagihara, N. Takada, H. Suda, Chem. Phys. Lett. 565 (2013) 138–142.
[28] C. Shan, J.B.P. Soares, A. Penlidis, Polymer 43 (2002) 767–773.
[29] R. Dastjerdi, M. Montazer, Colloids Surf., B: Biointerfaces 79 (2010) 5.
[30] Z. Huang, P.C. Maness, D.M. Blake, E.J. Wolfrum, S.L. Smolinski, W.A. Jacoby, J. Photochem. Photobiol., A: Chem. 130 (2000) 163–170.
[31] K. Sunada, T. Watanabe, K. Hashimoto, J. Photochem. Photobiol., A: Chem. 156 (2003) 227–233.
[32] J.R. Gurr, A.S.S. Wang, C.H. Chan, K.Y. Jam, Toxicology 2013 (2005) 66–73.
[33] L.K. Adams, D.Y. Lyon, P.J.J. Alvarez, Water Res. 40 (2006) 3527–3532.